Three-dimensional sub-grain mapping of elastic strain state and orientations in the bulk of polycrystals

Péter Reischig, Wolfgang Ludwig

Three-dimensional sub-grain mapping of elastic strain state and orientations in the bulk of polycrystals

Péter Reischig[1,2], Wolfgang Ludwig[1,3]

[1] European Synchrotron Radiation Facility (71, avenue des Martyrs, CS 40220, 38043 Grenoble CEDEX 9, France)
[2] InnoCryst Ltd (CTH, Daresbury Laboratory, Sci-Tech Daresbury, Keckwick Lane, Daresbury, Warrington, WA4 4AD, United Kingdom)
[3] Laboratoire Materiaux, Ingenierie et Science, INSA Lyon, Université de Lyon (92, rue Pasteur, CS 30122, 69361 Lyon cedex 07, France)

Corresponding author's e-mail address: ludwig@esrf.fr

Abstract. Detailed information on the sub-grain deformation state in polycrystals at the micrometre scale and below is essential to fully understand a vast variety of interplay between microstructure and mechanical properties. We demonstrate the possibility of efficiently mapping the complete local strain tensor, including hydrostatic strain, at the sub-grain level in three dimensions inside a polycrystal, along with the local crystal orientations and crystal structure, in a non-destructive way. The resulting three dimensional maps have a strain resolution in the order of 10^{-4}, spatial resolution in the order of micrometres, and can cover several hundred micrometres in size and include hundreds or thousands of grains. Datasets are obtained via Diffraction Contract Tomography (DCT), where the effects of the grain shapes and the deformation fields are convoluted in the recorded diffraction spots. The grain shapes and the local sub-grain crystal orientation and strain information is inferred in a novel data processing approach using a forward model and an iterative non-linear solver. The method uses a parallel, monochromatic synchrotron X-ray beam and the scan consists of a single rotation of the specimen, enabling short scanning times and a robust setup. The challenges in achieving high spatial, orientation and strain resolution, and of the mathematical problem of resolving the local deformation are described, and preliminary validation test results are presented.

1. Introduction

Mapping the deformation state in polycrystals at the sub-grain level enables valuable insight into the underlying mechanics of key material processes and provides validation for modeling. Current synchrotron and laboratory based X-ray methods have only delivered limited spatially resolved crystallographic information due to multiple shortcomings, e.g. low spatial resolution, low penetration, low or no strain sensitivity, too small volumes or too long measurement times, restricted geometry, restrictions in grain size or mosaicity, or an unstable experimental setup. There is no efficient method for mapping sub-grain strain state in volumes extending over a large number of grains in all three dimensions.

While EBSD is limited to the surface, high energy X-rays, from 20keV upwards, provide both penetration and strain sensitivity in common metallic alloys. 3DXRD [1] and related synchrotron X-ray based methods [2,3,4] employ monochromatic X-ray beams with energies typically above 30 keV. They can provide grain average properties, including the grain average strain tensor, often even in

highly deformed grains, by analysing the positions of diffraction spots from individual grains on an area detector [2,5,6]. Grain maps, showing grain shapes, grain boundaries [7] and local orientations [8,9], can be obtained using a high spatial resolution detector and irradiating the specimen with a beam of a rectangular or a line cross-section. Lens-based X-ray dark-field microscopy [10] can map specific strain components inside grains at 100nm spatial resolution with a complex experimental setup.

In X-ray micro-diffraction [11,12] a polychromatic pencil beam is scanned laterally and a wire is scanned in the diffracted beam to obtain a three-dimensional map at sub-micron resolution and up to a few tens of micrometers depth. Deviatoric strain is measured at 10^{-4} accuracy, and accessing the hydrostatic component requires scanning the photon energy in a reflection, resulting in a very lengthy process.

In this work, we present a novel data processing method for Diffraction Contrast Tomography (DCT), or similar techniques, that has the capability of efficiently mapping the complete strain tensor (five deviatoric and one hydrostatic component) at the sub-grain level in three dimensions inside a polycrystal, along with the local crystal orientations and crystal structure, in a non-destructive way. The experimental implementation utilises a full beam approach where the entire gauge volume is irradiated simultaneously with a monochromatic synchrotron beam, and several (hkl) reflections are recorded from each grain. Since it requires scanning only a single axis, the method is robust and very efficient in terms of scanning time, which enables studying samples in-situ in consecutive scans.

2. Experimental procedure and data processing

2.1. Experimental setup and spatial resolution

While the DCT experimental setup is relatively simple (Figure 1) and can be easily implemented on a micro-tomography station, the calibration and data processing is challenging as the effects of the grain shapes and the deformation fields are convoluted in the recorded diffraction spots. The basic method is routinely available on the ID11, BM5 and possibly other beamlines at the ESRF. The data processing steps are described in [6]. The sample is rotated continuously over 360°, and the diffracted beams in the dark beam area of the detector are integrated in small angular steps of typically 0.05°, resulting in a dataset of 7200 images. The diffraction spots that originate from the grains are stored as a (u,v,ω) 3D volume: u and v being the horizontal and vertical image coordinates, and ω is the rotation angle. The diffraction spots are indexed according to grains, and the individual grain shapes are reconstructed. The 3D grain map is assembled from the grains. The spatial resolution comes directly from the spatial resolution of the detector: typically 0.7 to 5um pixel size is used. An advanced version of DCT can account for and resolve a misorientation distribution within the grains [9].

2.2. DCT scan on a gum metal specimen under tensile load

Preliminary results on a polycrystalline gum metal sample with a composition of Ti-36Nb-2Ta-3Zr-0.3O wt% and mean grain diameter of 61um are presented. Gum metal is able to sustain elastic strains up to 1.5% elongation and above. The specimen was scanned with DCT, using 40keV beam energy, 1.5sec exposure time per image, 0.05° ω angular step size, resulting in 7200 images. The detector pixel size was 1.4um, and the rotation axis to detector distance was 7mm. To allow for the detector read-out time, the rotation stage was turned back to the correct starting position for each image, so that gaps in the integration were avoided. The total scan time was 5h. A uniaxial tensile stress of approximately 350MPa was applied to the sample during the scan. Nearly all diffraction spots belonged to the first four{hkl} families.

2.3. Achieving strain sensitivity

Although it seems counterintuitive to use a high resolution detector close to the sample for strain measurements, the small pixel-size still provides a suitable orientation, and thus, strain resolution. As the number of pixels (1000 to 4000) is similar in a far-field (as in 3DXRD) and a near-field detector, the diffraction angle range covered is also comparable, though typically less {hkl} plane families are

recorded in a DCT dataset. In the DCT setup described above, the orientation sensitivity in the scattering vectors (i.e. the plane normals) is $6.5*10^{-4}$rad per pixel and $6.2*10^{-4}$rad per image for a diffraction spot at three quarters along the diagonal from the centroid towards a corner of the detector. The small ω rotational stepping is adapted to the bandwidth of the energy spectrum of the X-ray beam, and it contributes directly to the orientation accuracy. For example, an 0.05° ($8.7*10^{-4}$rad) ω stepping matches well a monochromatic bandwidth of 10^{-3} dE/E band width used typically on the ID11 beamline of the ESRF. Table 1 shows the highest deformation sensitivity in one of the Gum metal grains. Recording 20 to 100 reflections from a crystal enables resolving orientation and strain components of a scattering vector with a few times 10^{-4} accuracy. Undistortion correction is applied to the raw images to compensate for the distortion introduced by the visible light optics of the detector, based on the X-ray or visible light image of a regular grid.

u (10^{-4} / pixel)			**v (10^{-4} / pixel)**			**ω (10^{-4} / rotation step)**		
* 9.8	19.6	604.2	447.9	459.5	* 9.6	16.4	* 9.0	53.0
20.8	* 10.4	536.5	569.4	396.1	* 10.3	* 8.7	16.5	62.8
11.3	13.5	279.6	296.9	264.2	* 10.0	* 3.9	* 5.7	31.7

Table 1 Maximum sensitivity to the 3x3 deformation tensor components of the (u,v,ω) dimensions in all 45 detected diffraction spots of a Gum metal grain. The highest sensitivity (lowest value) for each component is marked by an asterisk.

2.4. Calibration of the setup geometry

Calibrating the DCT setup geometry to the same level as the expected strain accuracy (down to 10^{-4}) is essential, and more challenging due to the small pixel sizes and distances, as using the powder standards that are commonly used for far-field detectors is not effective, and the setup on the beamline is not permanent. Consequently, the calibration is usually done from the dataset itself, although an additional DCT scan of a well-known undeformed polycrystal standard or an assemble of single crystals could be considered.

2.4.1. Geometry calibration based on Friedel pairs

There is usually a significant error in the estimate of the initial rotation axis to detector distance, hence also in the diffraction angles. As a first step, Friedel pairs of diffraction spots are found 180° ω offset based only the intensity and size of the spots. In a Bragg angle vs azimuthal angle plot the {hkl} families are clearly visible as lines, and the detector distance, tilts and lateral offset can approximately be set manually. In a next step, now taking into account the Bragg and azimuthal angles, the Friedel pairs are matched and grouped into {hkl} families automatically. The detector distance and tilts, and optionally the beam energy or lattice parameters are found in an automatic non-linear iterative optimisation procedure, where the deviation between the applied incident X-ray wavelength and wavelengths computed from the Friedel pairs is minimised in a least squares sense. All the grains are assumed to have zero strain at this stage, i.e. the nominal lattice parameters. Even at significant elastic strains (10^{-2} level), the accuracy in the setup geometry achieved here is sufficient to index the observed diffraction spots and find the grains.

2.4.2. Global fitting

After the indexing step, when the grain positions and orientations are known, the (u,v,ω) positions of the centroids of the observed reflections can be compared with their expected positions on the detector which are computed via forward modelling. With the forward model usually the following parameters are fitted simultaneously in a non-linear least squares optimization: the grain centroid positions, mean orientations, mean strain state; detector distance, lateral position, tilts; rotation axis wedge angle. In addition, the model can take into account sample drifts. The beam energy, effective detector pixel size and the zero-strain nominal lattice parameters are usually fixed. The grain orientation and strain

accuracy increases with an increasing number of diffraction spots indexed, and a few times 10^{-4} precision is achievable.

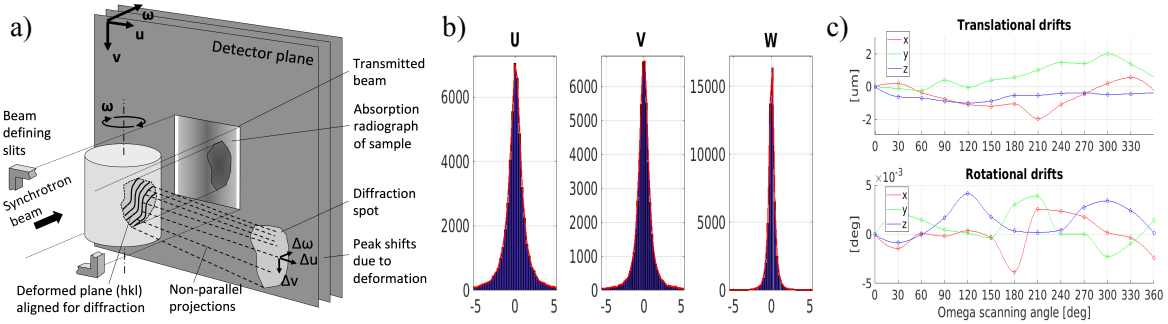

Figure 1 a) DCT setup and peak shifts due to deformation. b) Results of the global fitting in Gum metal. Histogram of (u,v,ω) errors between observed and forward simulated diffraction spot centroid positions after fitting. c) Fitted translational and rotational drifts of the sample during the scan.

2.5. Scanning times and stability

The typical length of a DCT scan is 1 to 12 hours, depending on the level of deformation in the sample, the sample material, i.e. the X-ray energy used, and as with any other method, the required spatial resolution. In case of lighter materials, such as aluminium or titanium, and smaller pixel sizes, scan times as low as tens of minutes is achievable. The ongoing upgrade of the storage ring at the ESRF to the Extremely Brilliant Source is expected to deliver an order of magnitude improvement in scanning times at ID11. Shorter scanning times automatically translate into higher stability of the sample and setup during a scan or a series of scans. In-situ experiments that involve mechanical loading or heating carry an even higher risk of the sample drifting during the scan.

The global fitting procedure described above can now take into account slow sample drifts during the scan. The drifts of the sample are described in the forward model with three translational and three rotational degrees of freedom of a rigid body over time, i.e. at a set of ω angles (vertices), usually at fixed ω intervals, e.g. at every 15°. The first vertex point is ω=0° at the start of the scan, where the drifts by definition are zero, and where the grain positions and orientations are defined and fitted. The last ω vertex is at the end of the scan at ω=360°. In the interim regions, the drift values are computed by interpolation, normally a shape preserving piece-wise cubic method. The drift values affect every diffraction spot position throughout the scan, just like the setup geometry parameters. The detector positions and the wedge angle of the rotation axis should be fitted in a first stage, then kept fixed when the sample drifts are fitted, otherwise the fitted setup parameters are not unique and a pseudo rotation axis may be found with the corresponding sinusoidal sample drifts, which can be confusing. When the drifts are found to be well below the detector pixel size, they can be neglected to simplify further processing. Otherwise, they could be taken into account in the forward simulation model used for shape and deformation reconstruction.

Beyond the increased accuracy, the ability to determine sample drifts increases the confidence in the results, and can help salvage datasets or entire experiments. Furthermore, it can also help correct for certain cases of hardware miscalibration which result in a systematic measurement error, e.g. a rotation synchronisation problem.

2.6. Inferring spatial, orientation and deformation information

The shape and the local orientation and strain fields are sought in each grain independently after the indexing step. Grain shape is modelled as a binary 3D volume, allowing for concave shapes. One grain in a DCT map typically consists of 10 to 200 voxels along one dimension. A local deformation tensor with 9 unknown components describe the local deviation from the mean grain lattice orientation and strain in each voxel, and determine the deviation of the diffracted beam direction relative to the grain mean. As the local deformation changes, the voxel projects into a slightly different (u,v,ω) location

and pixel in every one of its (hkl) diffraction spots. The diffracted intensity from a voxel is distributed over the eight pixels nearest to its (u,v,ω) location, i.e. a 2x2x2 region in (u,v,ω) in each diffraction spot. The intensities from all the voxels are summed to generate the forward projection of each diffraction spot, following kinematical scattering theory.

Since the deformation field is unknown, so is the projection geometry, which leads to a large ill-posed, non-linear problem, which is challenging to solve. Regular 3D reconstruction techniques are not applicable, and the voxels may project relatively far (several pixels away) from the zero strain position. The solution for the shape and deformation field is found by minimising the intensity differences between a grain's measured and simulated diffraction spots over (u,v,ω) in an iterative optimisation. In the current implementation, the grain shape and deformation field reconstruction is alternated. Firstly an initial grain shape is obtained with a Simultaneous Iterative Reconstruction Technique (SIRT) algorithm, as in the usual DCT processing [4], assuming a fixed zero local deformation field, thus a fixed projection geometry throughout the grain, which can be treated as a linear problem. The diffraction spots are integrated along ω into 2D (u,v) projections to be used as input in the shape reconstruction. Secondly the deformation field is sought at a fixed grain shape. Then the shape and deformation solution is sought in an alternating manner, whilst keeping the other one fixed.

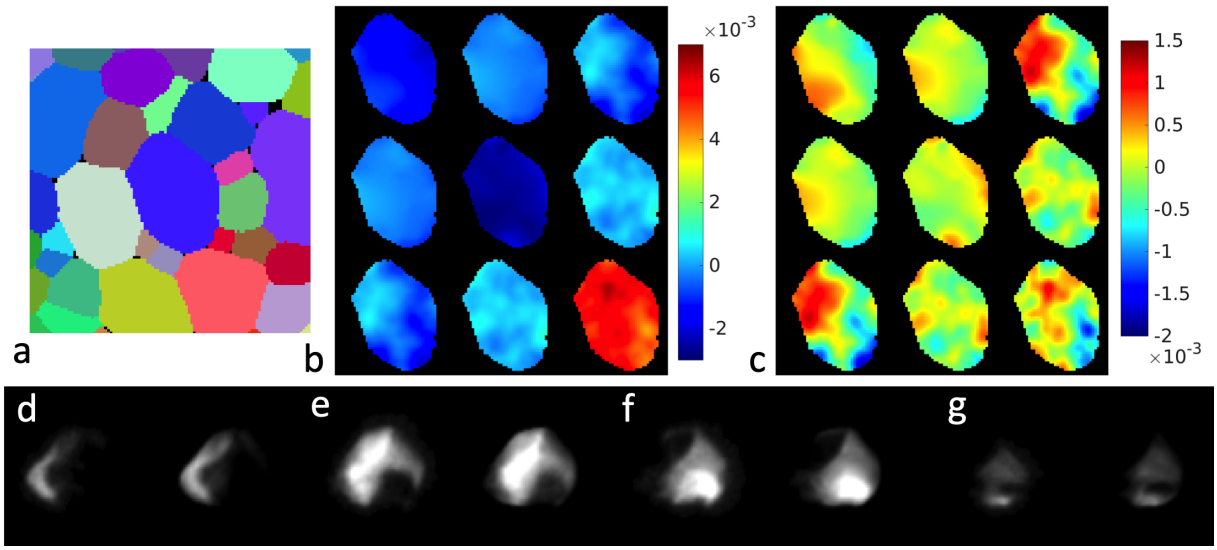

Figure 2 a) Detail of a horizontal slice of the grain map of gum metal, showing reconstructed grain shapes in a neighbourhood. b) Resolved absolute strain components within the central blue grain. c) Deviation of resolved strain values from the grain average. d-g) Segments in (u,v) of one of the diffraction spots of the grain at four consecutive ω steps; measured (left) and forward simulated (right). The voxel size in the reconstruction is 2.5um.

In each stage, the deformation tensor components are found in an iterative optimisation which is linearised for a small number of iterations, and formulated in a way that a SIRT or conjugate gradient method can be applied to improve the solution according to:

$$\Delta\mathbf{d}^* = \underset{\Delta\mathbf{d}}{\operatorname{argmin}} \left\| \frac{\partial \mathbf{p}}{\partial \mathbf{d}} \Delta\mathbf{d} - \Delta\mathbf{p} \right\|_2^2$$

where **d** is a vector of all nine deformation components of all voxels, **Δd*** is the next correction to update **d**, **p** is a vector containing the intensity of all the pixels where any of the voxels project, **Δp** is the difference between the observed and simulated intensities in the last iteration. The deformation solution is smoothed regularly during the iteration, which serves as regularisation. Preliminary testing shows that the optimisation can find the deformation field in certain setup geometries and deformation states. The local deformation solution is then combined with the grain mean orientation and strain, and

then decomposed into three local crystal orientation and six local strain components (the left stretch tensor) via polar decomposition.

3. Results and discussion

The global fitting was applied to 1500 indexed grains of the gum metal sample. Figure 1b shows histograms of the residual errors in the (u,v,ω) spot centroid positions before and after the fitting. They are close to one pixel and one rotational step, and come from background noise, segmentation errors and overlaps. The fitted sample drifts, shown in Figure 1c, are below one pixel and 10^{-4} rad, hence in this case are negligible.

The shape and local deformation reconstruction reached convergence for a large number of grains, and the simulated and observed diffraction spots show close resemblance (Figure 2) in the intensity distributions over (u,v,ω). The grain shapes and strain values seem realistic, and the mean strain state corresponds to the tensile load that was applied perpendicular to the cross-section presented. The processing time was tens of minutes to hours per grain on multicore computers. The reliability and applicability of the strain retrieval algorithm and the accuracy of the resulting strain maps require further investigation. It is best adapted to moderate deformation gradients, and large plastic deformations may prevent it from finding a solution.

4. Conclusions

The kinematical vector model, a single deformation state per voxel and summing diffracted intensities from all voxels to simulate diffraction spots, in 3DXRD and DCT type experiments appears to be a good and effective approximation for polycrystals of metals. Using a near-field detector and a full beam approach, such as DCT, can provide sufficient strain sensitivity and a robust and very efficient scanning procedure to obtain 3D grain maps with sub-grain strain information on moderately deformed grains. It is possible to decompose the shape, orientation and strain information in the diffraction spots via large scale iterative optimisation.

Acknowledgements

The authors thank Dimitris Karkoulis, Nicola Vigano, Andrew King, Max Langer, José Baruchel, Jürgen Härtwig, Tilo Baumbach, Jon Wright and Shigeru Kuramoto for their input and fruitful discussions during the course of this study, and the ESRF for providing beamtime on beamline ID11.

References

[1] Poulsen H F 2004 *Three-Dimensional X-ray Diffraction Microscopy; Mapping Polycrystals and Their Dynamics* (Berlin: Springer)
[2] Bernier J V, Barton N R, Lienert U and Miller M P 2011 *J. Strain Anal. Eng.* **46,** 527–547
[3] Suter R M, Hennessy D, Xiao C and Lienert U 2006 *Rev. Sci. Instrum.* **77** 123905
[4] Ludwig W, Reischig P, King A, Herbig M, Lauridsen E M, Johnson G, Marrow T J and Buffière J Y 2009 *Rev. Sci. Instrum.* **80** 033905
[5] Oddershede J, Schmidt S, Poulsen H F, Sørensen H O, Wright J and Reimers W 2010 *J. Appl. Cryst.* **43** 539–549
[6] Reischig P, King A, Nervo L, Vigano N, Guilhem Y, Palenstijn W J, Batenburg K J, Preuss M and Wolfgang L 2013 *J. Appl. Crystallogr.* **46** 297–311
[7] Schmidt S, Olsen U L, Poulsen H F, Sørensen H O, Lauridsen E M, Margulies L, Moris C and Juul Jensen D 2008 *Scr. Mater.* **59,** 491–494
[8] Li S F and Suter R M 2013 *J. Appl. Crystallogr.* **46** 512–524
[9] Vigano N, Tanguy A, Hallais S, Dimanov A, Bornert M, Batenburg K J, and Ludwig W 2016 *Scientific Reports* **6**:20618
[10] Simons H, King A, Ludwig W, Detlefs C, Pantleon W, Schmidt S, Stöhr F, Snigireva I, Snigirev A and Poulsen H F 2015 *Nat. Comm.* **6**:6098
[11] Larson B C, Yang W, Ice G E, Budai J D and Tischler J Z 2002 *Nature* **415,** 887–890
[12] Larson B C and Levine L E 2013 *J. Appl. Cryst.* **46** 153–164